Half-Heusler topological insulators: A first-principles study with the Tran-Blaha modified Becke-Johnson density functional

Wanxiang Feng,[1] Di Xiao,[2] Ying Zhang,[3,4] and Yugui Yao[1,4]
[1]*Institute of Physics, Chinese Academy of Sciences, Beijing 100190, China*
[2]*Materials Science & Technology Division, Oak Ridge National Laboratory, Oak Ridge, Tennessee 37831, USA*
[3]*Department of Physics, Beijing Normal University, Beijing 100875, China*
[4]*Department of Physics, The University of Texas at Austin, Austin, Texas 78712, USA*
(Received 11 October 2010; published 15 December 2010)

We systematically investigate the topological band structures of half-Heusler compounds using first-principles calculations. The modified Becke-Johnson exchange potential together with local-density approximation for the correlation potential (MBJLDA) has been used here to obtain accurate band inversion strength and band order. Our results show that a large number of half-Heusler compounds are candidates for three-dimensional topological insulators. The difference between band structures obtained using the LDA and MBJLDA potential is also discussed.

DOI: 10.1103/PhysRevB.82.235121 PACS number(s): 71.15.Mb, 71.20.Nr, 73.20.At

I. INTRODUCTION

Motivated by their potential applications in spintronics and quantum computing,[1] the search for three-dimensional topological insulators (3DTI) has attracted considerable theoretical and experimental interest.[2–13] These materials are called "topological" because they are distinguished from ordinary insulators by the so-called Z_2 topological invariants associated with the bulk band structure.[14,15] On the theory side, the state-of-the-art first-principles calculations guided by topological band theory[16–18] has provided a powerful tool for uncovering new families of 3DTI. Based on this approach, it has been recently predicted that ternary half-Heusler compounds can realize the topological insulating phase with proper strain engineering.[11–13]

There are several ways to determine the band topology of an insulator. Intuitively, one can count the number of band inversions within the entire Brillouin zone—an *odd* number indicates that the material may be a 3DTI.[2,8] This method depends on an accurate interpretation of the atomic origin of the bands and is better suited for crystals with a high-symmetry lattice. A more rigorous method is to directly evaluate the Z_2 topological invariants. For materials with inversion symmetry, the parity criteria developed by Fu and Kane[2] can be readily applied. On the other hand, if the inversion symmetry is absent, one must resort to the more elaborated lattice computation of the Z_2 invariants.[19] We have recently applied this method to study the distorted half-Heuslers[11] and the noncentrosymmetric chalcopyrite compounds.[20] In practical calculations, both methods require an accurate knowledge of the bulk band structures. So far, previous works on 3DTI have employed either the local-density approximation (LDA) (Refs. 21 and 22) or generalized gradient approximation (GGA) (Ref. 23) for the exchange-correlation potential. However, it is well known that these approximations have the tendency to underestimate the band gap. In particular, if the material has a small positive band gap, this underestimation may yield a negative value. Therefore, these approximations may falsely predict an inverted band structure when the band order is actually normal.

Recently, a new semilocal potential that combines the modified Becke-Johnson (MBJ) exchange potential and the LDA correlation potential, called MBJLDA, was proposed by Tran and Blaha (Tran-Blaha) (Ref. 24) and aimed to obtain accurate band gaps and band order. The MBJLDA potential are computationally as cheap as LDA or GGA but it has similar precision compared with the more expensive hybrid functionals and GW method. It has been demonstrated[24] that the MBJLDA potential can be used to describe many types of solids, including wide band-gap insulators, small band-gap *sp* semiconductors, and strongly correlated 3*d* transition-metal oxides. More importantly, the MBJLDA potential can effectively mimic the behavior of orbital-dependent potential around the band gap, so it is expected to obtain accurate positions of states near the band edge, which are the keys to determine the band inversion and the band topology.

In this work we perform a systematic investigation of the band topology of the half-Heusler family using the MBJLDA potential, and compare it with the LDA result. The improved accuracy of the MBJLDA potential over LDA is tested in the ordinary insulator CdTe and the topologically nontrivial 3D-HgTe, whose band structures are known experimentally and can be used as a benchmark. We then focus on the ternary half-Heusler compounds. By calculating the band inversion strength, we confirm our previous prediction that a large number of half-Heuslers are possible candidates for 3DTI or 3D topological metal.[11] The difference between LDA and the MBJLDA potential is also discussed and a clear discrepancy is found between these two methods. The sensitivity of the calculated band structure due to the type of exchange-correlation potential calls for more detailed experimental works.

II. METHOD

The band-structure calculations in this work were performed using full-potential linearized augmented plane-wave method,[25] implemented in the package WIEN2K.[26] A converged ground state was obtained using 10 000 k points in

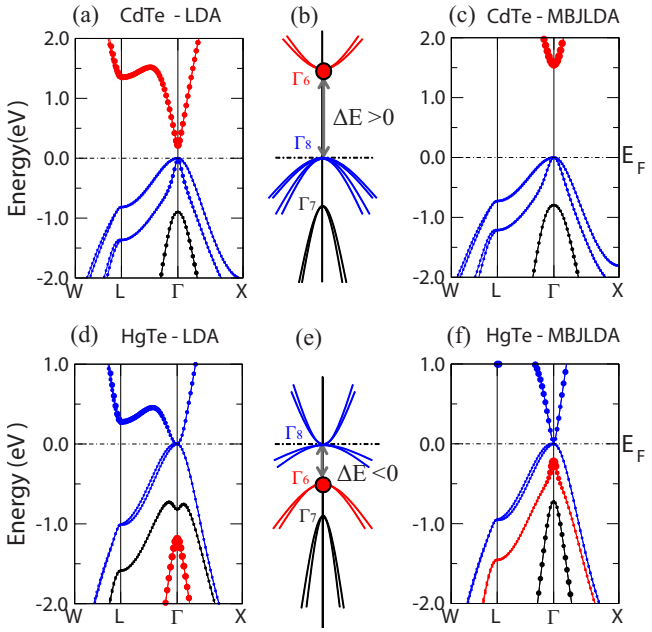

FIG. 1. (Color online) Band structure of CdTe and HgTe. (a) LDA and (c) MBJLDA results of CdTe; (d) LDA and (f) MBJLDA results of HgTe. The Γ_6, Γ_7, and Γ_8 state are denoted by red, black, and blue color, respectively. The size of dots is proportional to the probability of *s*-orbit projection. (b) and (e) is schematically experimental band structure of CdTe and HgTe, the red solid dots denote the *s*-orbit originated Γ_6 state. The band inversion strength is defined as $\Delta E = E_{\Gamma_6} - E_{\Gamma_8}$. The calculated and experimental energy of Γ_6, Γ_7, and Γ_8 state are listed in Table I.

the first Brillouin zone with $K_{max}R_{MT}=9.0$, where R_{MT} represents the smallest muffin-tin radius and K_{max} is the maximum size of reciprocal-lattice vectors. Wave functions and potentials inside the atomic sphere are expanded in spherical harmonics up to $l=10$ and 4, respectively. Spin-orbit coupling is included by a second-variational procedure,[25] where states up to 9 Ry above Fermi level are included in the basis expansion, and the relativistic $p_{1/2}$ corrections were also considered for $5p$ and $6p$ orbit in order to improve the accuracy.[27]

III. RESULTS AND DISCUSSIONS

A. CdTe and HgTe

We first test the MBJLDA potential for the binary compounds CdTe and HgTe. The energy bands of both compounds at the Γ point near the Fermi-level split into Γ_6 (twofold degenerate), Γ_7 (twofold degenerate), and Γ_8 (fourfold degenerate) states due to the zinc-blende crystal symmetry and strong spin-orbit interaction. The experimental band order of CdTe and HgTe are (from high to low energy) Γ_6, Γ_8, Γ_7 (Refs. 28 and 29) and Γ_8, Γ_6, Γ_7 (Ref. 30), respectively. They are schematically shown in Figs. 1(b) and 1(e). From the viewpoint of band topology, the main difference between these two compounds is that CdTe possesses a normal band order, i.e., the *s*-like Γ_6 state sits above the *p*-like Γ_8 state, while HgTe possesses an inverted band order in which the Γ_6 state is occupied and sits below the Γ_8 state. We then define the band inversion strength ΔE as the energy differences between these two states, i.e.,

$$\Delta E = E_{\Gamma_6} - E_{\Gamma_8}. \quad (1)$$

A negative ΔE typically indicates that the materials are in a topologically nontrival phase, while those with a positive ΔE are in a topologically trivial phase.

Figure 1 shows the LDA and MBJLDA band structures of CdTe and HgTe at their experimental lattice constants 6.48 Å and 6.46 Å, respectively.[31] The calculated energy of the Γ_6, Γ_7, and Γ_8 states together with their experimental values are listed in Table I. For CdTe, the LDA potential yields a serious underestimation of ΔE. For HgTe, it obtains the wrong band order of the Γ_6 and Γ_7 states (but it does predict an inverted band order). On the other hand, the MBJLDA result shows an excellent agreement with experiments for both compounds. We therefore conclude that the MBDLDA potential is better suited to calculate the topological band structure.

TABLE I. The energy of Γ_6, Γ_7, and Γ_8 state of CdTe and HgTe calculated with LDA and MBJLDA at their experimental lattice constants 6.48 Å and 6.46 Å, respectively (Ref. 31). Experimental values are also shown for comparison. The Fermi level are always located on Γ_8 state, and E_{Γ_8} are set to zero. The energy units are electron volt.

		LDA	MBJLDA	Experiment
CdTe	$E_{\Gamma 6}$	0.221	1.549	1.475[a]
	$E_{\Gamma 8}$	0.0	0.0	0.0
	$E_{\Gamma 7}$	−0.897	−0.795	−0.95[b]
HgTe	$E_{\Gamma 8}$	0.0	0.0	0.0
	$E_{\Gamma 6}$	−1.191	−0.234	−0.29[c]
	$E_{\Gamma 7}$	−0.822	−0.721	−0.91[c]

[a]Reference 28.
[b]Reference 29.
[c]Reference 30.

B. Half-Heuslers

Having established the improved accuracy of the MBJLDA potential over LDA, we now turn to the ternary half-Heusler compounds described by space group $F\bar{4}3m$. The chemical formula of these materials is *XYZ*, where *X* and *Y* are transition or rare-earth metals and *Z* a heavy element. It can be regarded as a hybrid compound of *XZ* with rocksalt structure, and *XY* and *YZ* with the zinc-blende structure (see Fig. 2). In our band-structure calculations, the lattice constants are taken from experimental data library.[32,33] For compounds without experimental lattice constant, we use the value obtained by total-energy minimization in first-principles calculations.

The band structures of half-Heuslers are very similar to CdTe/HgTe. In particular, the low-energy electron dynamics is dominated by energy bands at the Γ point. Therefore, the band topology of half-Heuslers can be characterized by the

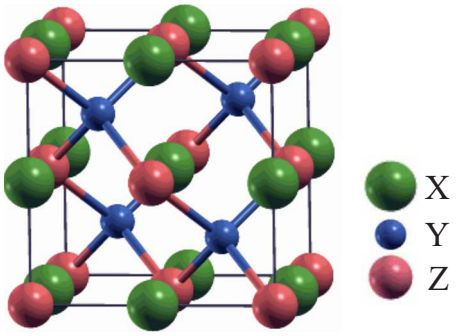

FIG. 2. (Color online) Crystal structure of half-Heusler compound *XYZ* in the $F\bar{4}3m$ space group, where *X* and *Y* are transition or rare-earth metals and *Z* a heavy element. Green spheres at (0.5,0.5,0.5) are atom *X*, dark blue spheres at (0.25,0.25,0.25) are atom *Y*, and pink spheres at (0,0,0) are atom *Z*. It can be regarded as a hybrid compound of *XZ* with rocksalt structure, and *XY* and *YZ* with the zinc-blende structure

band inversion strength ΔE defined in Eq. (1). In order to systemically explore their topological phase, we have calculated ΔE by both LDA and MBJLDA for 24 half-Heusler compounds, as shown in Figs. 3(a) and 3(b), respectively. Following our previous work (Ref. 11), we have also calculated the Z_2 invariant for all half-Heusler compounds investigated here. The calculated Z_2 invariant agrees with the intuitive band inversion picture, that is, materials with negative ΔE are in topologically nontrivial phase. As shown in Fig. 3(b), we have identified nine half-Heusler compounds, LuPtSb, LaPtBi, YPtBi, ScPtBi, ThPtPb, LaAuPb, YAuPb, LuPdBi, LuPtBi as possible candidates for topological insulators or topological metal. (Note that ScPtBi, ThPtPb, LaAuPb here are virtual compounds.) Here, the band structures of the first six compounds are with zero band gap similar to that of HgTe, and the last three compounds possess the nontrivial metallic band structures similar to Fig. 4(e) or the conduction bands droping below the Fermi level near the X point.

As shown in Sec. III A, the LDA result generally yields a smaller value of the band inversion strength ΔE when compared with the MBJLDA result, which agrees much better with the experimental data. We emphasize that, unlike the usual energy gaps, here ΔE can take on both positive and negative values, hence a positive ΔE is always larger than a negative one. This trend is also confirmed for half-Heuslers. As shown in Fig. 3, ΔE by MBJLDA is always larger than that by LDA. In particular, if LDA calculation predicts a small negative ΔE, it may become positive when using MBJLDA potential, such as ScAuPb and YPdBi. This suggests that when predicting topological phases, one must be careful with the types of exchange-correlation potentials.

To illustrate the general difference between the LDA and MBJLDA results, we present four scenarios shown in Fig. 4 using some typical examples. Both LDA and MBJLDA calculations predict that LaPtBi [Figs. 4(a) and 4(b)] has an inverted band structure, which is very similar to HgTe. The main difference is the band order exchange between Γ_6 and Γ_7 state. Although the band topology will not change, the LDA result clearly underestimates the ΔE due to the downward movement of Γ_6 state. For YPdBi, the problem is much more severe as the two potentials give different band topology. As shown in Figs. 4(c) and 4(d), the LDA result shows an inverted band order but the MBJLDA result shows a normal band order. The two types of exchange-correlation potentials also affects the electronic behavior around the Fermi level as shown for YPtBi in Figs. 4(e) and 4(f). The metallic phase predicted by LDA calculation becomes a zero-band-gap semiconductor in MBJLDA calculation. The band order of Γ_6 and Γ_7 is also exchanged, just like LaPtBi.

As mentioned in our previous Letter (Ref. 11), the nontrivial topological phase can be generally realized by apply-

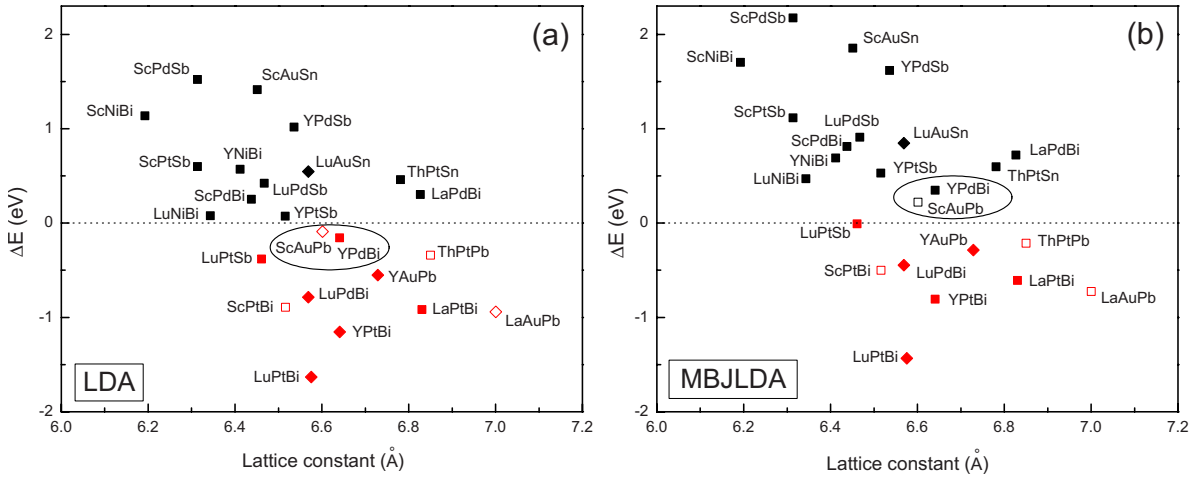

FIG. 3. (Color online) Band inversion strength of half-Heusler compounds calculated by (a) LDA and (b) MBJLDA. The materials with open symbols indicate that there is not experimental reports, and the lattice constant are obtained by first-principles total-energy minimization. The red squares mark the topological insulator candidates (after applying a proper uniaxial strain), red diamonds mark topological metals, black squares mark ordinary insulators, and black diamonds mark ordinary metals. The topological nontrivial phase is below the horizontal line while the trivial phase is above horizontal line. The materials enclosed by circle indicate that their topological phase predicted change by using different exchange-correlation potential.

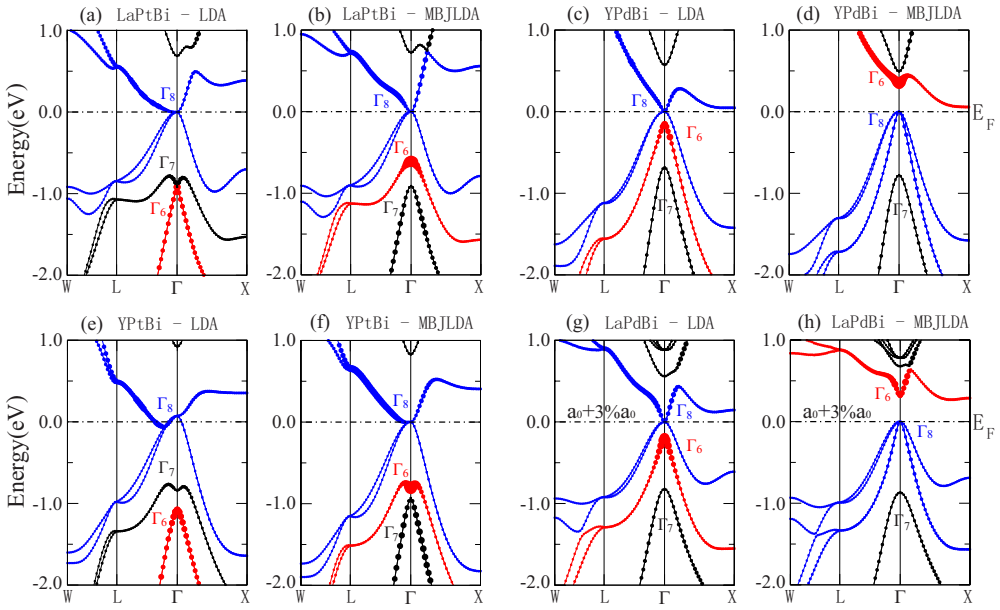

FIG. 4. (Color online) LDA and MBJLDA band structure of half-Heusler compounds LaPtBi (a) and (b), YPdBi (c) and (d), YPtBi(e) and (f), and LaPdBi (g) and (h). The Γ_6, Γ_7, and Γ_8 state are denoted by red, black, and blue color, respectively. The size of dots is proportional to the probability of *s*-orbit projection.

ing hydrostatic expansion to change the band order. For example, LaPdBi has normal band order in its native state [Fig. 5(a)], a 7% change in the lattice constant converts the trivial topological phase into a nontrivial topological phase [Fig. 5(b)]. The effect of volume expansion is that the effective positive charge of the Pd core is increased due to the delocalization of its *d* orbit. This causes the Pd *s* orbit to be more attracted by the Pd core, and consequently, the Γ_6 state (mainly from atom Pd *s* orbit) jumps below the Γ_8 state. This formation of band inversion is very similar to HgTe.[34] Conversely, the hydrostatic compression leads to opposite results. For example, YAuPb has inverted band order in its native state [Fig. 5(c)], a −5% change in lattice constant converts the nontrivial topological phase into a trivial topological phase [Fig. 5(d)]. We have calculated other small band-gap compounds under hydrostatic strain all of the results indicate that the hydrostatic expansion leads to a topological nontrivial phase, whereas the hydrostatic compression leads to a topological trivial phase. Again, there are different effects on the band order under the same hydrostatic strain when using different exchange-correlation potentials. For example, when one stretches lattice constant to $a=a_0+3\%a_0$, LDA calculation will yield an inverted band structure [Fig. 4(g)] while it still has a normal band order by MBJLDA calculation [Fig. 4(h)].

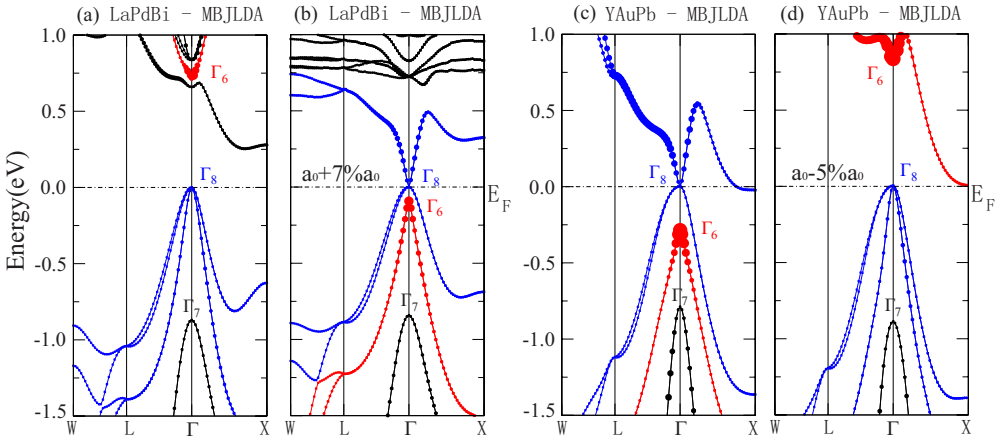

FIG. 5. (Color online) Band structures of LaPdBi and YAuPb by MBJLDA. (a) without and (b) with a 7% hydrostatic expansion of LaPdBi, (c) without and (d) with a 5% hydrostatic compression of YAuPb. The Γ_6, Γ_7, and Γ_8 state are denoted by red, black, and blue color, respectively. The application of a hydrostatic expansion in (b) causes the Γ_6 state to jump below the Γ_8 state, and leads to a nontrivial topological phase. In contrast, the application of a hydrostatic compression in (d) causes the Γ_6 state to jump above the Γ_8 state, and leads to a trivial topological phase.

IV. SUMMARY

In summary, we have systematically investigated the topological band structure of the half-Heusler family using both LDA and MBJLDA exchange-correlations potential. Our result shows that a large number of half-Heusler compounds are candidates for three-dimensional topological insulators. We also discussed the main differences between the LDA and MBJLDA potentials

Note added in proof: Recently, we became aware of a similar work about ternary half-Heusler compound.[35]

ACKNOWLEDGMENTS

This work was supported by NSF of China (Grants No. 10674163 and No. 10974231) and the MOST Project of China (Grant No. 2007CB925000), Welch Foundation (Grant No. F-1255) and DOE (Grant No. DE-FG02-02ER45958, Division of Materials Science and Engineering), and by Supercomputing Center of Chinese Academy of Sciences (SCCAS) and Texas Advanced Computing Center (TACC).

[1] J. E. Moore, Nature (London) **464**, 194 (2010).
[2] L. Fu and C. L. Kane, Phys. Rev. B **76**, 045302 (2007).
[3] D. Hsieh, D. Qian, L. Wray, Y. Xia, Y. S. Hor, R. J. Cava, and M. Z. Hasan, Nature (London) **452**, 970 (2008).
[4] H. Zhang, C.-X. Liu, X.-L. Qi, X. Dai, Z. Fang, and S.-C. Zhang, Nat. Phys. **5**, 438 (2009).
[5] Y. Xia, D. Qian, D. Hsieh, L. Wray, A. Pal, H. Lin, A. Bansil, D. Grauer, Y. S. Hor, R. J. Cava, and M. Z. Hasan, Nat. Phys. **5**, 398 (2009).
[6] Y. L. Chen, J. G. Analytis, J.-H. Chu, Z. K. Liu, S.-K. Mo, X. L. Qi, H. J. Zhang, D. H. Lu, X. Dai, Z. Fang, S. C. Zhang, I. R. Fisher, Z. Hussain, and Z.-X. Shen, Science **325**, 178 (2009).
[7] B. Yan, C.-X. Liu, H.-J. Zhang, C.-Y. Yam, X.-L. Qi, T. Frauenheim, and S.-C. Zhang, EPL **90**, 37002 (2010).
[8] H. Lin, R. S. Markiewicz, L. A. Wray, L. Fu, M. Z. Hasan, and A. Bansil, Phys. Rev. Lett. **105**, 036404 (2010).
[9] T. Sato, K. Segawa, H. Guo, K. Sugawara, S. Souma, T. Takahashi, and Y. Ando, Phys. Rev. Lett. **105**, 136802 (2010).
[10] Y. Chen, Z. Liu, J. Analytis, J. Chu, H. Zhang, S. Mo, R. Moore, D. Lu, I. Fisher, S. Zhang, Z. Hussain, and Z. Shen, arXiv:1006.3843 (unpublished).
[11] D. Xiao, Y. G. Yao, W. Feng, J. Wen, W. Zhu, X.-Q. Chen, G. M. Stocks, and Z. Zhang, Phys. Rev. Lett. **105**, 096404 (2010).
[12] H. Lin, L. A. Wray, Y. Xia, S. Xu, S. Jia, R. J. Cava, A. Bansil, and M. Z. Hasan, Nature Mater. **9**, 546 (2010).
[13] S. Chadov, X. Qi, J. Kübler, G. H. Fecher, C. Felser, and S. C. Zhang, Nature Mater. **9**, 541 (2010).
[14] C. L. Kane and E. J. Mele, Phys. Rev. Lett. **95**, 146802 (2005).
[15] L. Fu and C. L. Kane, Phys. Rev. B **74**, 195312 (2006).
[16] L. Fu, C. L. Kane, and E. J. Mele, Phys. Rev. Lett. **98**, 106803 (2007).
[17] J. E. Moore and L. Balents, Phys. Rev. B **75**, 121306 (2007).
[18] R. Roy, Phys. Rev. B **79**, 195322 (2009).
[19] T. Fukui and Y. Hatsugai, J. Phys. Soc. Jpn. **76**, 053702 (2007).
[20] W. X. Feng, J. Ding, D. Xiao, and Y. G. Yao, Phys. Rev. Lett. (to be published).
[21] W. Kohn and L. J. Sham, Phys. Rev. **140**, A1133 (1965).
[22] J. P. Perdew and Y. Wang, Phys. Rev. B **45**, 13244 (1992).
[23] J. P. Perdew, K. Burke, and M. Ernzerhof, Phys. Rev. Lett. **77**, 3865 (1996).
[24] F. Tran and P. Blaha, Phys. Rev. Lett. **102**, 226401 (2009).
[25] D. J. Singh, *Planewaves, Pseudopotentials and the LAPW Method* (Kluwer Academic, Boston, 1994).
[26] P. Blaha, K. Schwarz, G. Madsen, D. Kvaniscka, and J. Luitz, *Wien2k, An Augmented Plane Wave Plus Local Orbitals Program for Calculating Crystal Properties* (Vienna University of Technology, Vienna, Austria, 2001).
[27] P. Larson, Phys. Rev. B **68**, 155121 (2003).
[28] P. Lemasson, Solid State Commun. **43**, 627 (1982).
[29] D. W. Niles and H. Höchst, Phys. Rev. B **43**, 1492 (1991).
[30] N. Orlowski, J. Augustin, Z. Golacki, C. Janowitz, and R. Manzke, Phys. Rev. B **61**, R5058 (2000).
[31] J. C. Woolley and B. Ray, J. Phys. Chem. Solids **15**, 27 (1960).
[32] P. Villars and L. D. Calvert, *Pearson's Handbook of Crystallographic Data for Intermetallic Phases* (American Society for Metals, Metals Park, OH, 1991).
[33] SPRINGERMATERIALS—The Landolt-Bönstein Database, http://www.springermaterials.com/navigation/
[34] A. Delin and T. Klüner, Phys. Rev. B **66**, 035117 (2002).
[35] W. Al-Sawai, Hsin Lin, R. S. Markiewicz, L. A. Wray, Y. Xai, S.-Y. Xu, M. Z. Hasan, and A. Bansil, Phys. Rev. B **82**, 125108 (2010).